Surface properties and reactivity of Al_2O_3-supported MoO_3 catalysts in ethane oxidative dehydrogenation

E. Heracleous [a], A.F. Lee [b], I.A. Vasalos [a], and A.A. Lemonidou [a,*]

[a] *Department of Chemical Engineering, Aristotle University of Thessaloniki and Chemical Process Engineering Research Institute, PO Box 1517, University City, Thessaloniki 54006, Greece*

[b] *Department of Chemistry, University of Hull, Hull HU6 7RX, UK*

Received 10 December 2002; accepted 6 March 2003

The effect of MoO_3 loading on the properties and the catalytic performance of a series of alumina-supported molybdena catalysts (0–30 wt% MoO_3) was investigated in the oxidative dehydrogenation of ethane. The molybdena species on alumina were found to be amorphous at submonolayer coverages. At higher loadings, the formation of $Al_2(MoO_4)_3$ crystallites was detected by XRD. XPS revealed the existence of both Mo(VI) and Mo(V) sites on the catalyst surface, the concentration of which depends on the MoO_3 loading. In terms of catalytic performance, the activity increases with increasing loading in the submonolayer regime, decreasing for higher loadings. High selectivity to ethene is obtained even at relatively high conversion levels for catalysts exceeding monolayer coverage.

KEY WORDS: oxidative dehydrogenation; ethane; molybdena/alumina catalysts; XPS.

1. Introduction

During the past decade, extensive research effort has been devoted to the chemical conversion of light alkanes to alkenes. In spite of their low reactivity, the abundance of cheap alkanes underlines the economic interest in their exploitation. The oxidative dehydrogenation (ODH) of ethane to ethene is a particularly attractive alternative route, considering that the growth rate of ethene demand is estimated to increase by 4.8% per year [1]. Moreover, ODH is a method that has the potential to overcome the main constraints of the conventional method used for the production of ethene [2].

An effective catalyst for the oxidative dehydrogenation of light alkanes would be a stable catalytic material, able to activate the strong C–H bonds of the alkane and prevent the over-oxidation of the reactant and the formed alkene to carbon oxides. In order to achieve both high activity and selectivity, the oxygen on the catalyst surface should be neither too strongly bound (low activity) nor too mobile (high activity, low selectivity) [3]. Different types of catalysts have been successfully tested for lower alkanes: catalysts based on alkali and alkaline earth oxides, which show high selectivity for ethene at temperatures higher than 600 °C, and catalysts based on reducible oxides, mainly early transition metal oxides, which activate stable ethane at lower temperatures [4,5]. Over reducible oxide-based catalysts, the reaction proceeds via a classical redox cycle. As is well known, the catalyst performance depends on a number of factors, such as the chemical nature of the active oxygen species, the redox properties and the acid–base character, which in turn depend on transition metal loading, dispersion and support effects [6–9].

Supported molybdenum oxide catalysts have stimulated much research interest due to their activity in a number of processes, including selective oxidation of alkanes. Meunier *et al.* have studied the ODH of propane over molybdena catalysts supported on several oxides [10]. TiO_2-supported MoO_3 was found to be the most selective catalyst at a surface coverage exceeding monolayer. Chen *et al.* [11–13] have investigated the structure and reactivity of ZrO_2- and Al_2O_3-supported MoO_3 for the ODH of propane. The ODH of propane over MoO_3/Al_2O_3 catalysts with different MoO_3 loading was also studied by Abello and co-workers, who came to the conclusion that the catalytic properties are related to the coordination of the Mo species [14]. The effect of support and alkali doping of the molybdena species on SiO_2/TiO_2 mixed oxides for the ODH of both ethane and propane have been studied by Watson and Ozkan [7,15].

The nature and surface distribution of the molybdenum species on the catalyst depend strongly on the preparation conditions (impregnation procedure, molybdenum loading, drying and calcination conditions, nature of support, etc.) [7,12]. The dispersion of MoO_x on Al_2O_3 has been thoroughly studied using many structural characterization techniques. It is generally accepted that at low Mo surface densities (<5 Mo/nm^2), Mo species form two-dimensional polymolybdates, highly dispersed on the surface of alumina. At higher Mo surface densities (exceeding monolayer coverage), MoO_3 crystallites are formed at low treatment temperatures (<600 °C), while $Al_2(MoO_4)_3$, a stable thermodynamic

* To whom correspondence should be addressed.

1011-372X/03/0500-0047/0

phase, is formed at higher treatment temperatures [11]. Results have also shown that the density of the active sites on the catalyst surface, which depends on the support surface chemistry and the molybdena loading, plays an important role in the redox behavior of the catalyst [16] and consequently on the catalytic performance.

Our goal in this study was to examine the use of alumina-supported molybdena catalysts in regard to their performance for the ODH of ethane. To our knowledge, there are no other reported data in the open literature concerning the performance of MoO_3/Al_2O_3 catalysts in the ODH of ethane. The effect of the MoO_3 loading (5–30 wt%) on the physicochemical characteristics of the catalysts was investigated using several techniques. Surface area was measured using the BET N_2 adsorption method. X-ray diffraction (XRD) and X-ray photoelectron spectroscopy (XPS) were used to determine the structure and dispersion of the molybdena species supported on Al_2O_3 as a function of increasing MoO_3 loading. Reactivity studies with equimolar C_2H_6/O_2 feedstock ratio were performed at various reaction temperatures and contact times.

2. Experimental

2.1. Catalyst preparation

Alumina-supported molybdenum oxide catalysts were prepared by wet impregnation of γ-Al_2O_3 (Engelhard, SA = 183.9 m^2/g) with hot aqueous solutions of ammonium heptamolybdate, $(NH_4)_6Mo_7O_{24}{\cdot}4H_2O$ (Fisher), to ensure full dissolution of the precursor. Prior to impregnation, the support was crushed and sieved to a particle size of 106–180 μm. The weight loading of MoO_3 varied between 5 and 30%. After impregnation, the solvent was removed by evaporation under reduced pressure and the resulting solid was dried overnight at 120 °C and calcined in synthetic air at 650 °C for 6 h. Supported molybdenum catalysts are referred to as xMoAl, where x indicates the wt% of MoO_3 related to weight of catalyst.

2.2. Catalyst characterization

The amount of molybdenum in the samples was measured by the inductively coupled plasma technique using a Plasma 400 Perkin-Elmer spectrometer. Surface areas of the samples were determined by N_2 adsorption at 77 K, using the multipoint BET analysis method, with an Autosorb-1 Quantachrome flow apparatus. Prior to the measurements, the samples were dehydrated in vacuum at 250 °C overnight. The crystalline structure of the catalysts was studied by XRD analysis with a Siemens D500 diffractometer, using Cu K_α radiation. XPS measurements were performed using a Kratos AXIS HSi instrument equipped with a charge neutralizer and an Mg K_α X-ray source. Spectra were recorded at normal emission using an analyzer pass energy of 20 eV, and X-ray power of 225 W. Apart from catalytic samples, spectra of bulk MoO_3 and $Al_2(MoO_4)_3$ were also recorded under identical conditions. Binding energies are referenced to adventitious carbon at 285 eV.

2.3. Measurements of catalytic performance

The catalytic performance of the samples was measured in a fixed-bed quartz reactor. The catalyst particles were diluted with an equal amount of quartz particles of the same size to achieve isothermal operation. The temperature in the middle of the catalytic bed was measured with a coaxial thermocouple. The samples were activated in flowing oxygen at 500 °C for 30 min. The composition of the reaction mixture used was $C_2H_6/O_2/He = 5/5/45$.

The ODH of ethane was investigated in the temperature range from 450 to 600 °C. For the determination of the activity of the catalysts as a function of temperature, the weight of the sample was 0.3 g and the total flow was 55 cm^3/min. In order to obtain different ethane conversion levels at constant reaction temperature the W/F ratio was varied from 0.2 to 1.08 g s/cm^3. The reaction products were analyzed on line by a Varian 3400 gas chromatograph equipped with a thermal conductivity detector (TCD). Three columns in a series-bypass configuration were used in the analysis: a 20% BEEA–20% DC 200/500, a Porapak N-Chromosorb 106 and a MS 5A. The main reaction products were C_2H_4, CO_2, CO and H_2O. Negligible amounts of oxygenates were observed at the reactor exit. The ethane conversion and the selectivity to the reaction products were calculated on a carbon basis. Closure of the carbon mass-balance was better than ±1%.

The contribution of gas-phase initiated reactions was tested by conducting experiments using an empty-volume reactor. The conversion of ethane at these experiments was lower than 2%, confirming that gas-phase reactions are negligible under the experimental conditions used for the activity tests.

3. Results and discussion

3.1. Catalyst characterization

The composition and the physicochemical characteristics of the supported molybdena catalysts are presented in table 1. The MoO_x surface coverage of the samples was calculated on catalyst surface area, as a fraction of a theoretical monolayer, using 22 $Å^2$ as the mean surface area occupied by one Mo^{6+} oxide unit on γ-Al_2O_3 [14]. Theoretical surface coverage values from 0.26 to 2.07 were obtained for the prepared catalytic samples.

Table 1
Physicochemical characteristics of the catalytic samples

Catalyst	MoO_3 loading (wt%)		BET surface area (m^2/g)	Theoretical surface coverage, θ
	Nominal	ICP analysis		
5MoAl	5	4.80	185.7	0.26
10MoAl	10	9.45	178.2	0.55
15MoAl	15	14.78	160.8	0.88
20MoAl	20	20.25	124.0	1.25
30MoAl	30	29.26	100.2	2.07

The specific surface area of the catalysts was found to decrease gradually with increasing molybdena content, from 185.7 m^2/g for the 5MoAl catalyst to 100.2 m^2/g for the 30MoAl catalyst. This decrease could be attributed to the blocking of the narrower pores of the support in accordance with literature data [14].

Crystalline phases in *x*MoAl catalysts were characterized by XRD. The diffractograms obtained are presented in figure 1. All samples exhibited diffraction lines characteristic of the γ-alumina support. No diffraction lines corresponding to Mo-containing compounds were detected in samples with MoO_3 loading up to 15 wt%, indicating that the molybdena species are amorphous in nature and highly dispersed on the surface of alumina. Higher MoO_3 loadings led to the appearance of lines corresponding to aluminum molybdate, $Al_2(MoO_4)_3$. These results are in agreement with studies of the thermal decomposition of ammonium heptamolybdate (the precursor salt for the preparation of the catalysts) in the presence of a γ-Al_2O_3 support. According to these studies, calcination of catalysts with a high molybdena loading at 550 °C leads to the formation of the crystallized orthorhombic MoO_3 phase, whereas calcination at 700 °C leads to the disappearance of the MoO_3 phase and the appearance of $Al_2(MoO_4)_3$ [17].

XPS was used to provide information about the oxidation state and the chemical environment of the

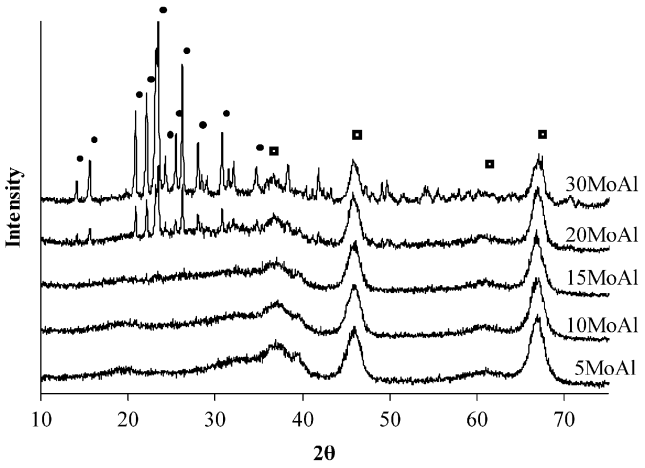

Figure 1. X-ray diffraction patterns of MoO_3/Al_2O_3 catalysts. The peaks are marked as (●) $Al_2(MoO_4)_3$ and (□) Al_2O_3.

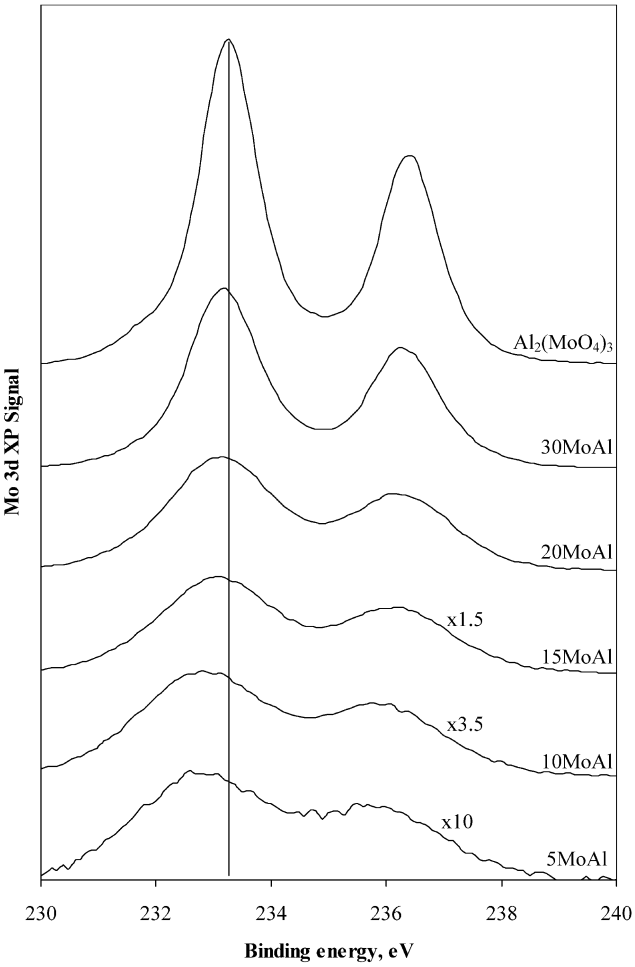

Figure 2. Mo 3*d* XPS spectra of MoO_3/Al_2O_3 catalysts with different MoO_3 loadings.

elements present on the surface of the catalysts. Figure 2 shows background-subtracted Mo 3*d* XP spectra for the series of *x*MoAl catalysts as a function of increasing MoO_3 loading. The spectrum of $Al_2(MoO_4)_3$ is also included for comparison. All spectra show doublets centered around 233 eV binding energy (Mo $3d_{5/2}$ component) with a spin–orbit splitting of 3.1 eV. The peak intensities show a strong increase with loading (figure 2), together with a progressive shift to higher binding energy as shown in table 2. This observation is in agreement with the data reported by Nag for MoO_3/Al_2O_3 catalysts [18]. Contradictory results appear in the literature about the dependence of the Mo 3*d* binding energy on the MoO_3 content. It has been reported that irrespective of the MoO_3 loading, the binding energy of the Mo doublet remains constant [19,20]. On the other hand, there are articles reporting that binding energy decreases [21] or increases with increasing MoO_3 loading [18,22].

The shift of the Mo 3*d* binding energy with loading is consistent with a structural change, such that the spectrum of the 30MoAl sample closely resembles that of either bulk $Al_2(MoO_4)_3$ powder or MoO_3. Unfortunately, XPS binding energies alone cannot differentiate

Table 2
XPS binding energies, full width at half maximum (FWHM) values and percentage of each oxidation state for the MoO_3/Al_2O_3 catalysts and reference samples

Catalyst	Mo $3d_{5/2}$ binding energy (eV)	Mo $3d_{5/2}$ FWHM (eV)	Percentage of each oxidation state	
			Mo(VI)	Mo(V)
5MoAl	232.79	2.54	66.5	33.5
10MoAl	232.84	2.43	69.5	30.5
15MoAl	233.09	1.95	75.5	24.5
20MoAl	233.14	1.70	84.5	15.5
30MoAl	233.20	0.97	100	0
MoO_3	233.23	0.79	100	0
$Al_2(MoO_4)_3$	233.23	0.79	100	0

between the two pure phases. The Mo 3*d* and O 1*s* binding energies obtained from XP spectra of reference materials MoO_3 and $Al_2(MoO_4)_3$ are indistinguishable. However, in our case since XRD shows only the existence of the mixed Mo–Al phase, we assign the Mo $3d_{5/2}$ peak obtained at 233.2 eV to $Al_2(MoO_4)_3$. The shift of the Mo 3*d* binding energy with increasing loading is accompanied by a decrease of the full width at half maximum (FWHM) values of the Mo $3d_{5/2}$ peak (table 2). The FWHM values approach that of the pure reference $Al_2(MoO_4)_3$ phase as the MoO_3 content increases. This remark is in line with data reported by other researchers [18–20].

Broadening and/or shifting of the Mo 3*d* binding energy has been ascribed to the different degree of interaction and the electron transfer between MoO_3 and support [18–21]. In our case, best fitting of the experimental XPS envelopes was achieved with two individual Mo $3d_{5/2}$ and Mo $3d_{3/2}$ doublets. Spectral deconvolution reveals the presence of two distinct Mo environments, with associated doublets located at 233.2 and 232 eV. The former can be assigned to Mo in a high oxidation state, Mo(VI), while the latter is indicative of Mo(V) sites [19]. As an example, the Mo 3*d* spectra of the 10MoAl and 20MoAl catalysts are shown in figure 3, with the deconvolution curves of the Mo $3d_{5/2}$ and Mo $3d_{3/2}$ signals originating from Mo(VI) and Mo(V). A striking transition from a 1:2 mixture of Mo(V):Mo(VI) to a pure Mo(VI) surface is apparent with increasing molybdenum loading, as clearly shown in table 2. The population of partially reduced Mo species on the catalyst surface strongly depends on the MoO_3 loading. We speculate that alumina is able to stabilize Mo species at a reduced state even after calcination under aerobic conditions. Indications for the presence of reduced Mo species on the surface of fresh catalysts have been also reported in the literature [23–25].

The ratio of the Mo 3*d* and Al 2*p* XPS signals can be used qualitatively as an indicator of the dispersion of the active phase on the surface of the catalyst. In figure 4 the XPS peak intensity ratio, I_{Mo}/I_{Al}, is plotted as a function

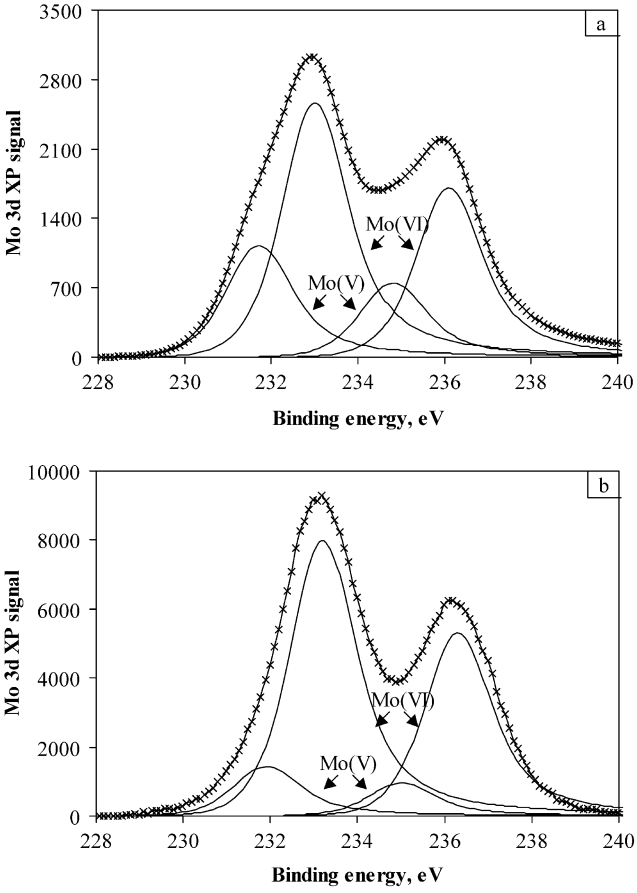

Figure 3. Deconvolution of the Mo 3*d* spectrum: (a) 10 wt% MoO_3/Al_2O_3; (b) 20 wt% MoO_3/Al_2O_3.

of the MoO_3 loading of the samples. A linear increase is observed up to 20 wt% MoO_3 loading, indicating a good dispersion of the molybdenum phase on the surface of the support. For the 30MoAl catalyst, a sharp non-linear increase of the I_{Mo}/I_{Al} ratio is observed. The increased value of this ratio is ascribed to the formation of $Al_2(MoO_4)_3$ crystallites. This observation supports the XRD results that revealed the presence of large

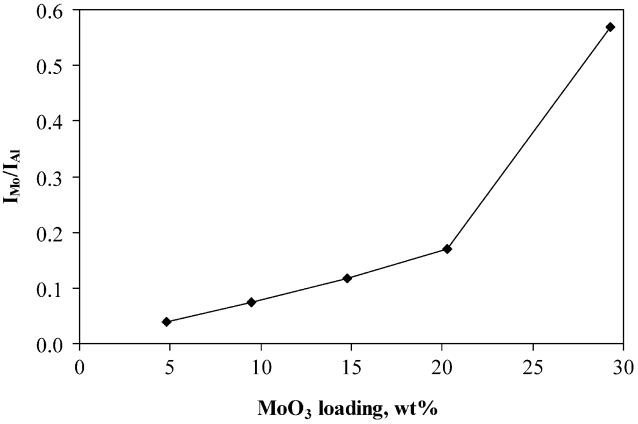

Figure 4. Intensity ratio of the XPS signals of Mo 3*d* and Al 2*p* as a function of MoO_3 content.

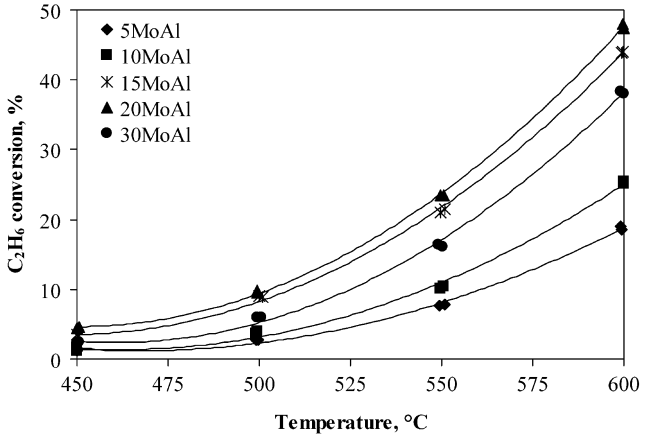

Figure 5. Ethane conversion as a function of temperature (reaction conditions: $W/F = 0.33\,g\,s/cm^3$, $C_2H_6/O_2 = 1:1$).

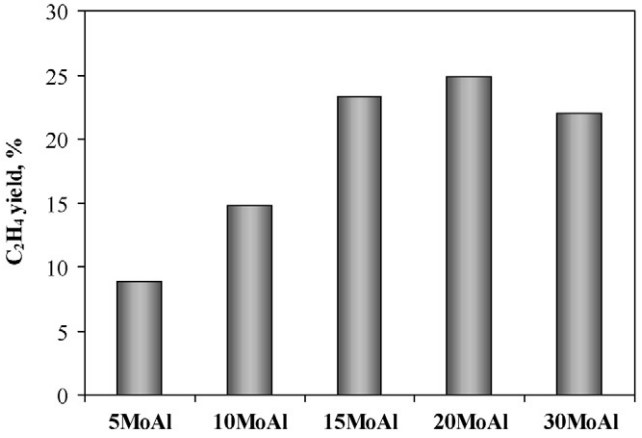

Figure 6. Yield of ethene for MoO_3/Al_2O_3 catalysts with different MoO_3 loadings (reaction conditions: $T = 600\,°C$, $W/F = 0.33\,g\,s/cm^3$).

$Al_2(MoO_4)_3$ crystals on the surface of the 30MoAl catalyst.

3.2. Catalytic results

The MoO_3/Al_2O_3 catalysts were tested for their efficiency in the ODH of ethane by performing two series of experiments.

In the first series, the activity of the catalysts was measured as a function of reaction temperature. The experiments were run at a temperature range of 450–600 °C, with a constant gas flow (55 cm^3/min), weight of catalyst (0.3 g) and ethane/oxygen ratio (1:1). The conversion of ethane is plotted in figure 5 as a function of reaction temperature. As expected, the activity of the samples increased with increasing temperature. Conversions of ethane up to 48% at 600 °C were observed with the 20MoAl catalyst. The corresponding oxygen conversion did not exceed 80%. The results clearly indicate that increasing the MoO_3 loading has a positive effect on the activity, which increases to a maximum at 20 wt% molybdena loading, decreasing at 30 wt%. These results are in agreement with reports in the literature for the catalytic performance of Mo-supported catalysts in the ODH of ethane and propane [7,10,11,14].

Apart from high activity, the molybdena catalysts are quite selective so as to produce high yields of ethene. The ethene yields obtained at the maximum temperature used in this series of experiments, 600 °C, are presented in figure 6. The yield of ethene increases from 8.8 to 25% over the 5MoAl and 20MoAl catalysts respectively. A slight decrease in ethene yield is observed with the 30MoAl catalyst.

Besides activity, selectivity to the corresponding alkene is of paramount importance for the evaluation of ODH catalysts. Since selectivity is strongly related to conversion, we conducted a second series of experiments at constant temperature (550 °C), constant ethane/oxygen ratio (1:1) and varying W/F from 0.2 to 1.08 g s/cm^3 in order to obtain different conversion levels. As depicted in figure 7 (conversion versus W/F), the increase of the W/F ratio results in improved activity for all the catalysts under study. Catalyst 20MoAl again proved the most active, since it attains a 10% conversion of ethane at 0.11 g s/cm^3, while three times higher W/F ratios are necessary for the 5MoAl catalyst to achieve the same conversion.

Figure 8 illustrates ethene selectivity as a function of ethane conversion. The results clearly demonstrate the inverse relation between selectivity and conversion, which is typical of the ODH reactions. Significant differences in ethene selectivity between the catalysts are observed. Ethene selectivity increases significantly with MoO_3 loading up to 15 wt%, while a further increase in MoO_3 content has negligible effect on selectivity. At low conversion levels, over 90% of ethane is converted to ethene over the 15MoAl, 20MoAl and 30MoAl catalysts. The presence of the stable mixed Mo–Al phase on the surface of the high-loading catalysts does not seem to affect selectivity. To verify the selectivity pattern of this phase, tests with pure $Al_2(MoO_4)_3$ at 650 °C showed that the mixed phase is very selective in ethane ODH

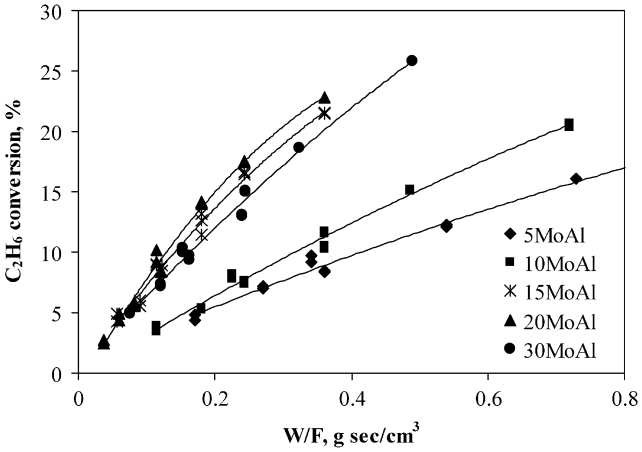

Figure 7. Ethane conversion as a function of W/F ratio (reaction conditions: $T = 550\,°C$, $C_2H_6/O_2 = 1:1$).

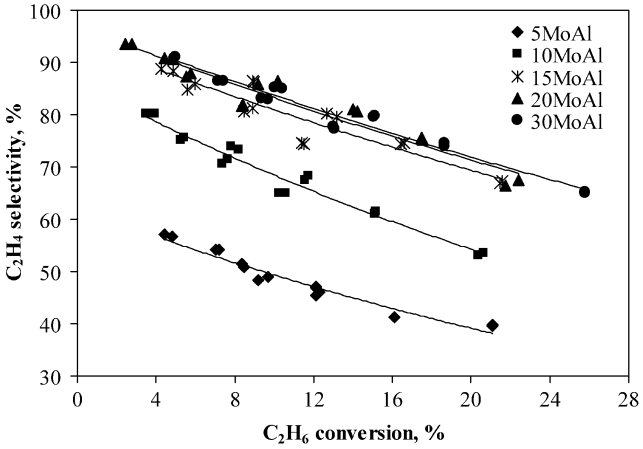

Figure 8. Ethene selectivity as a function of ethane conversion (reaction conditions: $T = 550\,^{\circ}C$, $C_2H_6/O_2 = 1:1$).

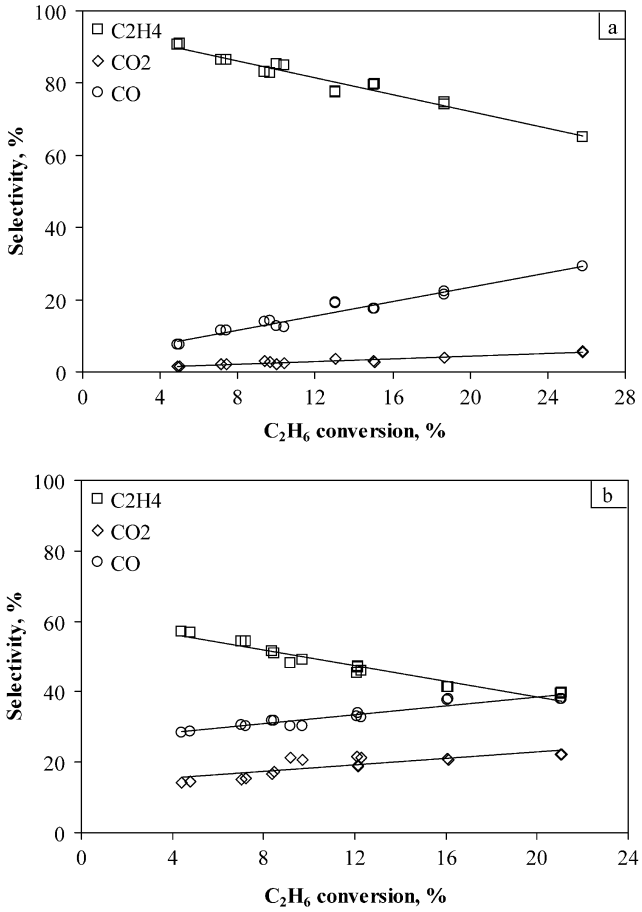

Figure 9. C_2H_4, CO_2 and CO selectivity as a function of ethane conversion (reaction conditions: $T = 550\,^{\circ}C$, $C_2H_6/O_2 = 1:1$): (a) 30 wt% MoO_3/Al_2O_3; (b) 5 wt% MoO_3/Al_2O_3.

with 91% ethene selectivity. Even though selectivity decreases with increasing conversion, the extent of secondary reactions is not significant. Ethene selectivity remains as high as 70% even at conversion levels around 25% over catalysts with a high molybdate surface coverage.

In order to get a clear picture of the reaction network, ethene selectivity together with CO and CO_2 selectivities as a function of ethane conversion are presented in figure 9 for the catalysts with the highest and lowest MoO_3 loading. In the presence of the 30MoAl sample (figure 9(a)) the selectivity toward CO and especially CO_2 at low conversion levels is very poor, indicating that the primary reaction that proceeds on the surface is that of dehydrogenation to ethene. It may be inferred that CO_x are formed almost exclusively from ethene via secondary oxidation reactions. The decrease in ethene selectivity is accompanied by an increase in the CO selectivity, while there is a very small variation of the CO_2 selectivity. It is thus clear that the main secondary reaction taking place is the oxidation of ethene to CO. Almost the same pattern is observed with 15MoAl and 20MoAl samples (not shown).

The dependence of CO_x and C_2H_4 selectivities on ethane conversion for the catalyst with the lowest MoO_3 content is depicted in figure 9(b). As is clearly shown, the relatively high selectivity to carbon oxides results not only from secondary oxidation of the alkene but also from primary unselective oxidation of ethane. Indeed, around 40% of initially reacting ethane is converted to CO_x. In contrast with high surface coverage catalysts, the ratio of CO/CO_2 remains almost constant over the whole conversion range, indicating that ethene is not preferentially oxidized to CO and/or the CO formed is rapidly oxidized to CO_2.

Chen *et al*. reported that initial selectivity to the olefin increases with increasing Mo surface density, until it reaches a constant value of 95% at surface densities higher than 5 Mo/nm^2. They claimed that Mo–O–Al sites or uncovered alumina surface near MoO_x species may catalyze the unselective conversion of propane to CO_x and that the complete coverage of the support by Mo species leads to high initial propene selectivity [11]. Even though these results cannot be directly related to our study, due to the different nature of the feedstock, the same trend of increasing selectivity with increasing Mo loading is observed in our catalytic experiments (figure 8). In order to check the effect of the bare support on the rate of unselective routes, tests were conducted with the support. Experimental results at various temperatures showed that alumina activates ethane, but even at low conversions (<5%), the selectivity to CO_x was over 85%. Thus, the influence of the support on product selectivity could explain the low ethene selectivity observed over catalysts with submonolayer coverages, as Chen *et al*. also proposed [11].

As evidenced by XPS, reduced Mo species are present on the surface and their concentration is strongly related to the MoO_x surface coverage (table 2). Studies in the literature suggest a correlation between the concentration of Mo(V) sites and propene yield in the propane ODH reaction [26]. Furthermore, it has been claimed that Mo(V) is the active site in propane ODH over

MoO_x-based catalysts [27]. Even though the presence of reduced Mo species on the catalysts under study was not determined under reaction conditions, where there is a dynamic equilibrium between reduced and oxidized species, the role of the different valence Mo surface species in the ODH reaction scheme cannot be neglected. The present results imply that the presence of a small amount of molybdena species in lower valence state favors the activation of ethane. Further studies are in progress in order to elucidate the effect of partially reduced Mo species and the structure of the MoO_x domains on the activity and selectivity of MoO_3/Al_2O_3 catalysts.

4. Conclusions

Characterization of 5–30 wt% MoO_3/Al_2O_3 catalysts shows that for loadings lower than that required for complete monolayer coverage, the molybdena species are two-dimensional and highly dispersed on the surface of alumina. At loadings above the monolayer, the formation of three-dimensional $Al_2(MoO_4)_3$ structures occurs, due to the strong interaction of Al and Mo and the high calcination temperature. The differing interaction of Mo species with the alumina support was evidenced by XPS measurements. The coexistence of Mo(VI) and Mo(V) sites on the outer surface layer has been verified for the fresh catalysts. A striking transition from a 1:2 mixture of Mo(V):Mo(VI) to a pure Mo(VI) surface is apparent with increasing molybdena loading.

Alumina-supported molybdena catalysts proved to be active and highly selective in the oxidative dehydrogenation of ethane to ethene. At loadings up to the monolayer, the activity of the samples increased with increasing MoO_3 content. Loadings corresponding to higher than the monolayer coverage lead to a decrease in catalytic activity, due to the growth of $Al_2(MoO_4)_3$ crystallites and/or the absence of small amounts of reduced Mo species. Selectivity to ethene increases with increasing loading up to 15 wt% ($\theta = 0.88$) and then remains constant. The results suggest that the best catalytic performance can be achieved with highly dispersed two-dimensional molybdenum species, fully encapsulating the alumina surface.

Acknowledgments

Dr. Lori Nalbandian from the Chemical Process Engineering Research Institute is acknowledged for the XRD and BET surface area measurements of the catalysts. Dr. K. Wilson from the University of York is acknowledged for the help with the XPS measurements.

References

[1] O&G Journal 95(2) (1997) 31.
[2] F. Cavani and F. Trifiro, Catal. Today 24 (1995) 307.
[3] H.H. Kung, Adv. Catal. 40 (1994) 1.
[4] G. Centi, F. Cavani and F. Trifiro, *Selective Oxidation by Heterogeneous Catalysis* (Kluwer Academic/Plenum Publishers, New York, 2001).
[5] M.A. Banares, Catal. Today 51 (1999) 319.
[6] T. Blasco and J.M. Lopez-Nieto, Appl. Catal. A 157 (1997) 117.
[7] R.B. Watson and U.S. Ozkan, J. Catal. 208 (2002) 124.
[8] A.A. Lemonidou, L. Nalbandian and I.A. Vasalos, Catal. Today 46 (2000) 333.
[9] M. Machli, E. Heracleous and A.A. Lemonidou, Appl. Catal. A 236 (2002) 23.
[10] F.C. Meunier, A. Yasmeen and J.R.H. Ross, Catal. Today 37 (1997) 33.
[11] K. Chen, S. Xie, A.T. Bell and E. Iglesia, J. Catal. 198 (2001) 232.
[12] K. Chen, S. Xie, A.T. Bell and E. Iglesia, J. Catal. 189 (2000) 421.
[13] K. Chen, S. Xie, A.T. Bell and E. Iglesia, J. Catal. 195 (2000) 244.
[14] M.C. Abello, M.F. Gomez and O. Ferretti, Appl. Catal. A 207 (2001) 421.
[15] R.B. Watson and U.S. Ozkan, J. Catal. 191 (2000) 12.
[16] H.M. Ismail, M.I. Zaki, G.C. Bond and R. Shukri, Appl. Catal. A 72 (1991) L1.
[17] A.A. Said, Thermochim. Acta 236 (1994) 93.
[18] N.K. Nag, J. Phys. Chem. 91 (1987) 2324.
[19] D.S. Zingg, L.E. Makovsky, E.R. Tischer, F.R. Brown and D.M. Hercules, J. Phys. Chem. 84 (1980) 2898.
[20] Y. Okamoto, H. Tomioka, Y. Katoh, T. Imanaka and S. Teranishi, J. Phys. Chem. 84 (1980) 1833.
[21] Y.V. Plyuto, I.V. Babich, I.V. Plyuto, A.D. Van Lagneveld and J.A. Moulijn, Appl. Surf. Sci. 119 (1997) 11.
[22] I. Rodriguez-Ramos, A. Guerrero-Ruiz, N. Homs, P. Ramirez de la Piscina and J.L.G. Fierro, J. Mol. Catal. A 95 (1995) 147.
[23] T.-J. Yang and J.H. Lunsford, J. Catal. 103 (1987) 55.
[24] J. Handzlik, J. Stoch, J. Ogonowski and M. Mikolajczyk, J. Mol. Catal. A: Chem. 157 (2000) 237.
[25] C. Fountzoula, N. Spanos, H.K. Matralis and C. Kordoulis, Appl. Catal. B: Environ. 35 (2002) 295.
[26] R.B. Watson and U.S. Ozkan, J. Phys. Chem. B 106 (2002) 6930.
[27] M.C. Abello, M.F. Gomez and L.E. Cadus, Catal. Lett. 53 (1998) 185.